

# Effect of Wavy Leading-Edges on Wings in Different Planetary Atmospheres

Vatasta Koul, Ayush Gupta, Vaibhav Sharma, Rajesh Yadav

**Abstract**—Today we are unmarking the secrets of the universe by exploring different stars and planets and most of the space exploration is done by unmanned space robots. In addition to our planet Earth, there are pieces of evidence that show other astronomical objects in our solar system such as Venus, Mars, Saturn's moon Titan and Uranus support the flight of fixed wing air vehicles. In this paper, we take forward the concept of presence of large rounded tubercles along the leading edge of a wing and use it as a passive flow control device that will help in improving its aerodynamic performance and maneuverability. Furthermore, in this research, aerodynamic measurements and performance analysis of wavy leading tubercles on the fixed wings at 5-degree angle of attack are carried out after determination of the flow conditions on the selected planetary bodies. Wavelength and amplitude for the sinusoidal modifications on the leading edge are analyzed and simulations are carried out for three-dimensional NACA 0012 airfoil maintaining unity AR (Aspect Ratio). Tubercles have consistently demonstrated the ability to delay and decrease the severity of stall as per the studies were done in the Earth's atmosphere. Implementing the same design on the leading edges of Micro-Air Vehicles (MAVs) and UAVs could make these aircrafts more stable over a greater range of angles of attack in different planetary environments of our solar system.

**Keywords**—Amplitude, NACA0012, tubercles, unmanned space robots.

## I. INTRODUCTION

THE nature has always served as a greatest and a unique source of inspiration even to the engineering world. An example that has intrigued fluid mechanists from a long time is of the humpback whale. Despite of its mammoth size, the mammal has the ability to around tight angles in its bubble-net feeding strategy [2]. Fish and Battle were the primary to postulate that the sinusoidal-shaped protuberances on the leading-edges of the whale's pectoral flippers, referred to as tubercles, may account for the humpback's extraordinary maneuverability through maintaining lift at high attack angles [1]. The motivation for investigating forefront protuberances on fluid dynamic control surfaces stems from the humpback whales' tubercles/scallops/sinusoidal perturbations/bumps interspersed along its leading edges. Despite its massive length and size, the whalebone whale is ready to execute complex underwater maneuvers and perform feats like rolls and loops. Since the flippers of a whalebone whale are a primary surface, it has been postulated that Leading edge (LE) tubercles on the

flippers are major contributors to the humpback whale's underwater agility [13]. Many engineering applications are associated with manufacturing methods involving the LEs of bluff and streamlined bodies.

Since it is well-known within the fluid dynamic literature, relatively small modifications near a number one edge can substantially alter, delay or reduce separation effects for wings, this can be most frequently achieved by protrusions like vortex generators that enhance physical phenomenon attachment. We demonstrate a concept that a wavy forefront can even enhance wing performance at a positive angle of attack even on different planets and might be used for future missions in space exploration. Over the past few years planetary science has made incredible advances by means of robotic missions meted out by spacecraft from our planet. Fly-by probes, orbiters, landers, hard probes/penetrators, rovers, and aerostats are launched, successfully completed their missions, and provided us invaluable data to expand our understanding of the scheme. Today, planetary science is poised to create further advances using robotic planetary aerial vehicles to conduct scientific investigations. During this study we have tried to produce insight into the mechanism chargeable for these benefits on earth likewise as other planetary objects in our scheme namely Venus, Mars, Earth, Saturn's moon Titan and Uranus.

## II. LITERATURE REVIEW

### A. Analogy from Humpback Whale

Humpback whale flippers are remarkable in many ways, including their curved planform, large AR, and surprising articulation, especially when compared with other whale species. Humpback whales naturally display LE tubercles that face into the free stream flow which further alters the fluid flow over these wings [5]. According to a research by Bushnell and Moore, it was contemplated that tubercles could be functional adaptations, thereby imparting an advantage in manoeuvrability and prey capture [14].

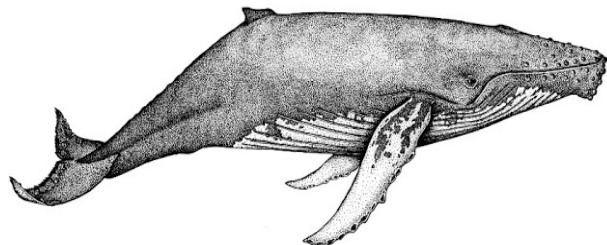


Fig. 1 Humpback Whale

Vatasta Koul, Vaibhav Sharma, Ayush Gupta are with the Department of Aerospace at University of Petroleum and Energy Studies, Dehradun 248007, Uttarakhand, India (e-mail: vatastakoul@gmail.com).

Rajesh Yadav is Assistant Professor, Dehradun, Uttarakhand, 248007.

### B. Tubercles

Flow control devices are commonly used on airfoils, hydrofoils, and wings to enhance their performance. These devices, whether passive or active, are designed to increase foil efficiency, stability, and/or reduce operational cost. There are many different types of devices aimed at achieving these goals, and some perform better than others. Recently, there has been a growing interest in a new type of flow control device, one which can be found in the natural world; tubercles. Tubercles are protuberances found on the LE of a Humpback whale pectoral flipper as shown in Fig. 1. They can be ideally characterized by two parameters, amplitude ( $A$ ) and wavelength ( $\lambda$ ), as shown in figure alongside. Note that for their size, the Humpback whale is incredibly agile, capable of underwater acrobatics. As seen in previous researches the tubercles on the LE of the Humpback whale may be responsible for the whale's agility [1]. It is now well known that when tubercles are placed on the LE of a foil or wing, the stall becomes more gradual and is typically delayed as per the researches done before. It should be noted that an airfoil means a two-dimensional lifting surface, whereas a wing will mean a finite or semi-finite lifting surface.

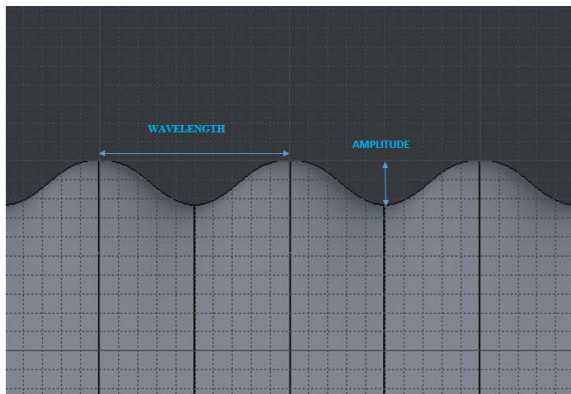


Fig. 2 The tubercles on the wing with the amplitude  $A = 0.06c$  and  $\lambda = 0.50c$

### C. Solar System Planetary Bodies

The purpose of the experimental investigation reported is to quantify the aerodynamic benefits of sinusoidal tubercles the selected airfoil at low Reynolds numbers at zero angle of attack on the different planetary bodies of our solar system to enhance the space exploration. The sun is heliocentric with all the planets orbiting the around it. It extends from the sun in the center to the inner rocky planets: Mercury, Venus, Earth and Mars and goes past the four gas giants Jupiter, Saturn, Uranus and Neptune. Along the timeline, we have even found ways and techniques to send off the various different satellites, rovers, telescopes and even human beings to outer space.

With the advancement in the technology, scientists are now developing and designing several different types of rotary and fixed wings which can be launched in the space and on other planets and such work has already been done on Mars and Venus. Due to this growth, there is a tendency to design and fabricate these types of drones and fixed wings which will



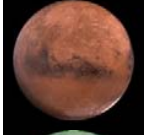
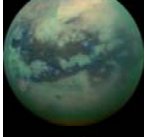

have the ability to explore and characterize the possible human landing sites. These will have the utmost advantage in the determining the appropriate or hazardous landing sites. In the near future, these drones can be used for inter-planetary mobility assists.

In addition to the planet Earth, there is an evidence that shows the other astronomical bodies in the solar system. The list of such bodies includes Venus, Mars, the gas giants, several moons and other bodies that have atmospheres, clouds and atmospheric dynamics. The selected planetary bodies differ with regard to its size, distance from the sun, gravity, atmospheric gases etc.

The Earth's atmosphere has a mixture of nitrogen, oxygen and some amount of water vapor, carbon dioxide and other gaseous molecules. On the other hand, the other planets have incredibly thin exospheres, whereas the gas giants have incredibly dense and powerful atmospheres. To broaden the basic understanding, the comparisons of these planetary atmospheres to Earth's atmosphere are made. In this section the atmospheric and physical features of the different targeted bodies are presented.

Table I discusses the atmospheric composition, gravity and respective wind speeds of the solar bodies since these are the necessary parameters for the computational methods.

TABLE I  
ATMOSPHERIC PROPERTIES OF SOLAR BODIES [10]-[12]

Planet	Image	Gravity ( $m/s^2$ )	Atmospheric gases Percentage Composition	Wind Speeds ( $m/s$ ) on planets
Venus		8.87	CO <sub>2</sub> - 96.5% N <sub>2</sub> - 3.5% SO <sub>2</sub> - 0.015%	100
Earth		9.81	N <sub>2</sub> - 78% O <sub>2</sub> - 21% Ar- 1%	4.96
Mars		8.71	CO <sub>2</sub> - 94.9% N <sub>2</sub> - 2.6% Ar- 1.9%	28
Titan		1.32	N <sub>2</sub> - 94.2% CH <sub>4</sub> - 5.65% H <sub>2</sub> - 0.015%	60
Uranus		8.69	H <sub>2</sub> - 83% He- 15% CH <sub>4</sub> - 2.3%	250

## III. NUMERICAL METHODOLOGY

## A. Conservation Equations

The purpose of the investigation reported is to study the aerodynamic characteristics of wings with LE tubercles in a commercial fluid flow solver using numerical analyses and governing equations using the finite volume methods. An incompressible flow is modelled using the Navier-Stokes equations which can be expressed as:

Navier-Stokes Equations:

Continuity:

$$\frac{\partial \rho}{\partial t} = -\left[\frac{\partial(\rho u)}{\partial x} + \frac{\partial(\rho v)}{\partial y} + \frac{\partial(\rho w)}{\partial z}\right] \quad (1)$$

X Momentum:

$$\frac{\partial u}{\partial t} = -u \frac{\partial u}{\partial x} - v \frac{\partial u}{\partial y} - w \frac{\partial u}{\partial z} + \frac{1}{\rho} \left[ -\frac{\partial p}{\partial x} + \frac{\partial \tau_{xx}}{\partial x} + \frac{\partial \tau_{yx}}{\partial y} + \frac{\partial \tau_{zx}}{\partial z} \right] \quad (2)$$

Y Momentum:

$$\frac{\partial v}{\partial t} = -u \frac{\partial v}{\partial x} - v \frac{\partial v}{\partial y} - w \frac{\partial v}{\partial z} + \frac{1}{\rho} \left[ -\frac{\partial p}{\partial y} + \frac{\partial \tau_{xy}}{\partial x} + \frac{\partial \tau_{yy}}{\partial y} + \frac{\partial \tau_{zy}}{\partial z} \right] \quad (3)$$

Z Momentum:

$$\frac{\partial w}{\partial t} = -u \frac{\partial w}{\partial x} - v \frac{\partial w}{\partial y} - w \frac{\partial w}{\partial z} + \frac{1}{\rho} \left[ -\frac{\partial p}{\partial z} + \frac{\partial \tau_{xz}}{\partial x} + \frac{\partial \tau_{yz}}{\partial y} + \frac{\partial \tau_{zz}}{\partial z} \right] \quad (4)$$

Energy:

$$\begin{aligned} \frac{\partial(e + \frac{v^2}{2})}{\partial t} = & -u \frac{\partial(e + \frac{v^2}{2})}{\partial x} - v \frac{\partial(e + \frac{v^2}{2})}{\partial y} - w \frac{\partial(e + \frac{v^2}{2})}{\partial z} + q + \frac{1}{\rho} \left[ \frac{\partial}{\partial x} \left( k \frac{\partial T}{\partial x} \right) + \right. \\ & \frac{\partial}{\partial y} \left( k \frac{\partial T}{\partial y} \right) + \frac{\partial}{\partial z} \left( k \frac{\partial T}{\partial z} \right) - \frac{\partial(pu)}{\partial x} - \frac{\partial(pv)}{\partial y} - \frac{\partial(pw)}{\partial z} + \frac{\partial(u\tau_{xx})}{\partial x} + \frac{\partial(u\tau_{yx})}{\partial y} + \\ & \left. \frac{\partial(u\tau_{zx})}{\partial z} + \frac{\partial(v\tau_{xy})}{\partial x} + \frac{\partial(v\tau_{yy})}{\partial y} + \frac{\partial(v\tau_{yz})}{\partial z} + \frac{\partial(w\tau_{xz})}{\partial x} + \frac{\partial(w\tau_{yz})}{\partial y} + \frac{\partial(w\tau_{zz})}{\partial z} \right] \quad (5) \end{aligned}$$

These equations have been written with the time derivatives on the left-hand side and all spatial derivatives on the right-hand side. This is the form suitable to the time dependent solution of the equation. These equations are partial differential equations that have a mathematically elliptic behavior that is, on a physical basis they treat flow field information and flow distribution that can travel throughout the flow field, in both upstream and downstream directions [8].

## B. Computational Model

The k-omega (k- $\omega$ ) SST (Shear Stress Transport) model formulation works from the inner part throughout the viscous sub-layers up till the walls. The k- $\omega$  SST can be used as a low Reynolds number flow application without extra damping functions. This model accounts for its good behavior in adverse pressure gradient and flow separation and does produce some large turbulence in regions with large normal strain such as the stagnation regions and the regions where the acceleration is strong.

The governing equations of the turbulent kinetic energy (k) and specific dissipation rate ( $\omega$ ) for the SST turbulence model

are obtained from a combination k- $\varepsilon$  and k- $\omega$  turbulence models which are read as [7]:

$$\frac{D(\rho k)}{Dt} = \nabla \cdot [(\mu + \sigma_k \mu_T) \nabla k] + P_k - \beta^* \rho \omega k \quad (6)$$

$$\begin{aligned} \frac{D(\rho \omega)}{Dt} = & \nabla \cdot [(\mu + \sigma_\omega \mu_T) \nabla \omega] + \gamma \frac{\rho}{\mu_T} P_k - \beta \rho \omega^2 + 2(1 - \\ & F_1) \rho \sigma_{\omega 2} \frac{(\nabla k) \cdot (\nabla \omega)}{\omega} \end{aligned} \quad (7)$$

where  $P_k = \min(\mu_T S2, 10\beta^* \rho k \omega)$ ; referred to as the production term. Functions and constants of the model are as follows:

$$F_1 = \tanh(\arg g_1^4) \quad (8)$$

$$\arg g_1 = \min \left[ \max \left( \frac{\sqrt{k}}{0.09 \omega d_w}, \frac{500 v}{d_w^2 \omega} \right), \frac{4 \rho \sigma_{\omega 2} k}{C D_{k\omega} d_w^2} \right] \quad (9)$$

$$C D_{k\omega} = \max \left( 2 \rho \sigma_{\omega 2} \frac{1}{\omega} \frac{\partial k}{\partial x_j} \frac{\partial \omega}{\partial x_j}, 10^{-10} \right) \quad (10)$$

$$F_2 = \tanh(\arg g_2^2) \quad (11)$$

$$\arg g_2 = \max \left( \frac{2\sqrt{k}}{0.09 \omega d_w}, \frac{500 v}{d_w^2 \omega} \right) \quad (12)$$

$$\sigma_k = F_1 \sigma_{k1} + (1 - F_1) \sigma_{k2} \quad (13)$$

$$\sigma_\omega = F_1 \sigma_{\omega 1} + (1 - F_1) \sigma_{\omega 2} \quad (14)$$

$$\beta = F_1 \beta_1 + (1 - F_1) \beta_2 \quad (15)$$

$$\gamma = \frac{\beta}{\beta^*} - \frac{\sigma_\omega \tau^2}{\sqrt{\beta^*}} \quad (16)$$

Coefficients of the model are read as [7]:  $\beta^* = 0.09$ ,  $\tau = 0.41$ ,  $\alpha_1 = 0.55$ ,  $\alpha_2 = 0.44$ ,  $\sigma_{k1} = 0.85$ ,  $\sigma_{k2} = 1.0$ ,  $\sigma_{\omega 1} = 0.5$ ,  $\sigma_{\omega 2} = 0.856$ ,  $\beta_1 = 0.075$ ,  $\beta_2 = 0.0828$ .

Eddy Viscosity function  $\mu_r = \frac{\rho \alpha_1 k}{\max(a_1 \omega, S F_2)}$  includes the so-called SST limiter, which is introduced so that the shear stress in the boundary layer under adverse pressure gradient can be prevented from over prediction. Therefore, the behavior of the model in such boundary layer, as well as separation on the suction side of the airfoil, is controlled by the  $\alpha_1$  constant. It is also responsible for modification and adjustment of flows around airfoil for SST model.

## C. Wing Geometry and Numerical Mesh

This research analyses the effect of tubercles on wing LE of NACA0012 and the impact on its aerodynamic properties. The cross-section profile of both plain LE and wavy LE are shown in Figs. 3 and 4 respectively. The final wing was modelled using CATIA (Dassault Systems) with their desired dimensions. The model was positioned such that the LE is located at the coordinate system while importing the model in Ansys mesh. The airfoil are full-span models have a mean chord of  $c = 200 \text{ mm}$  and a planform area of  $S = 800 \text{ mm}^2$ . The profiles located at smaller chord zones than the reference (valleys) have larger leading-edge radii and the profiles corresponding to maximum amplitude zones, displaying larger

chords (*peaks*), are relatively thinner than the reference geometry and have a smaller leading-edge radius. The amplitude and the wavelength of the sinus wave were fixed to  $0.06c$  and  $0.50c$ , respectively [3], [4]. The values used here for amplitude and wavelength are close to estimates taken from data of an actual humpback whale flipper and the previous done researches.

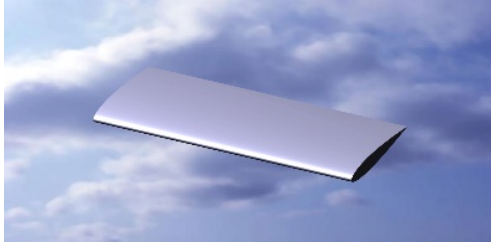


Fig. 3 NACA0012 with no leading-edge tubercles



Fig. 4 NACA0012 with LE tubercles

The method used for mesh is tetrahedrons with a body sizing of  $0.05$  m and face sizing of  $0.005$  m. Inflation layer with maximum of 11 layers and a growth rate of  $1.02$  is used for the analysis. The computational domain was made in Meshing (Fluent Inc./ANSYS) with a total of 508585 elements.

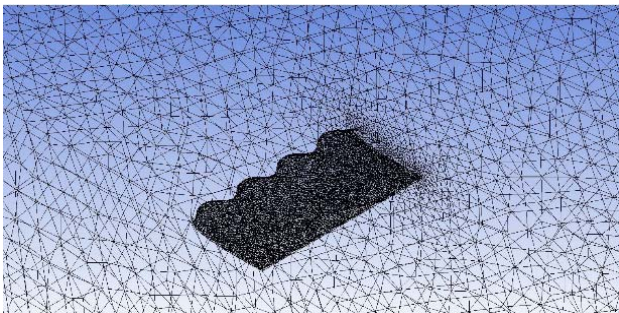


Fig. 5 Computational Mesh displayed on the wavy wing surface

In the model setup, pressure-based method is selected and for the materials, the species transport with different fluid databases is required as per the atmospheric properties of the particular solar body. The two-dimensional numerical simulations are conducted using commercially available finite volume solver with multi-species non-reacting mixture of gases as the working fluid to mimic the atmospheric condition of the different planets. Table II shows the mass fractions as

per the volumetric percentage of the atmospheric gases.

TABLE II  
MASS FRACTION OF GASES ON THE VARIOUS SOLAR BODIES

Planet	Composition of gases in Mass Fraction
Venus	CO <sub>2</sub> - 0.9772
	N <sub>2</sub> - 0.02256
	SO <sub>2</sub> - 0.00024
Mars	CO <sub>2</sub> - 0.9679
	N <sub>2</sub> - 0.0174
	Ar- 0.0147
Titan	N <sub>2</sub> - 0.96672
	CH <sub>4</sub> - 0.033203
	H <sub>2</sub> - 0.000077
Uranus	H <sub>2</sub> - 0.63314
	He- 0.22721
	CH <sub>4</sub> - 0.13963

#### IV. RESULTS AND DISCUSSIONS

To begin with, we validated the panel method by simulating the wing model in different planetary atmospheres using the commercially available solver with the mass species transport of mass fraction of the mixture of gases present on the particular planet. We then validated pressure contours on the various wing profiles on the different planetary bodies, by combining 2D measurements with basic airfoil theory on the effect of finite AR. It is observed that regions of low static pressures generated along the top of the wing (blue) result in generating lift. This further tapers off towards the wing tips and towards the trailing edge. The stagnation pressure region is shown as a red line underneath the LE of the wing [6]. For this simulation, the chord is  $c = 200$  mm,  $A = 0.06c$   $\lambda = 0.50c$  and the inlet velocity  $U_o = 15$  m/s (Subsonic Laminar Flow).

##### A. Venus

The atmosphere of Venus mainly consists of 96.5% carbon dioxide with 3.5% nitrogen and traces of sulphur dioxide making it ninety times denser than the planet earth. Due to the presence of the large amount of greenhouse gases, Venus has a hot and high-pressure environment near the surface, making the conditions possible for powered flight through its atmosphere.

The below done simulation for the wavy wing in the Venusian atmosphere justifies that it is possible to fly in the atmosphere of Venus. The pressure difference on the wing can be seen in the result obtained in Figs. 6 and 7.

##### B. Mars

The mars atmosphere majorly consists of carbon dioxide (around 95%), nitrogen (2.6%), argon (1.9%), traces of oxygen and water vapour. The pressure on the mars is very less compared to the earth atmosphere which changes from location to location around 600P a, density of the air is also less somewhere around  $0.012$  kg/m<sup>3</sup>, viscosity is  $1.14 \times 10^{-5}$  kg/ms, the average temperature of mars atmosphere is 260K and the speed of the sound is 256 m/s, the gravitational force is also less in the mars atmosphere which is around  $3.11$  m/s<sup>2</sup>. The pressure contours in the Martian atmosphere can be analyzed through the simulation.

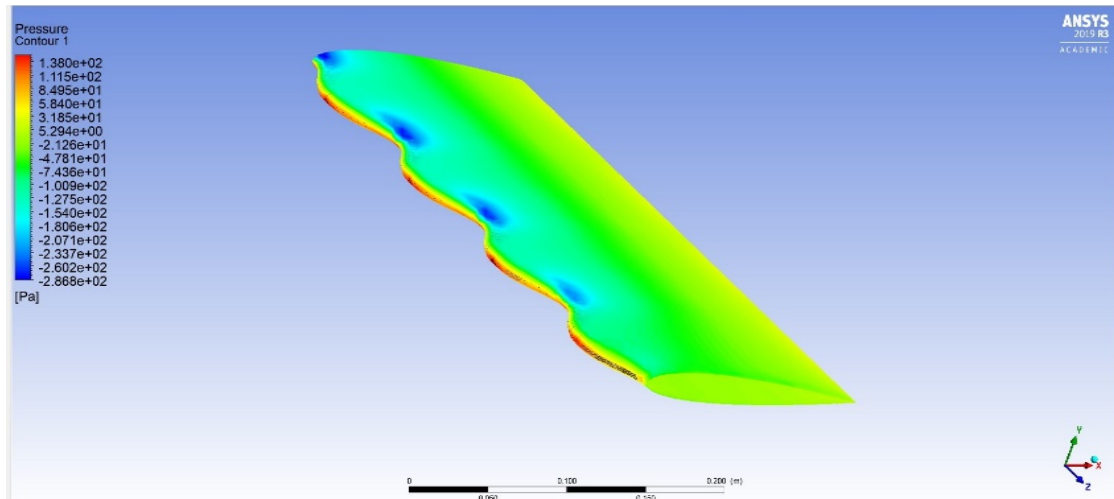


Fig. 6 Pressure contours on the wavy wing simulated in the Venusian atmosphere

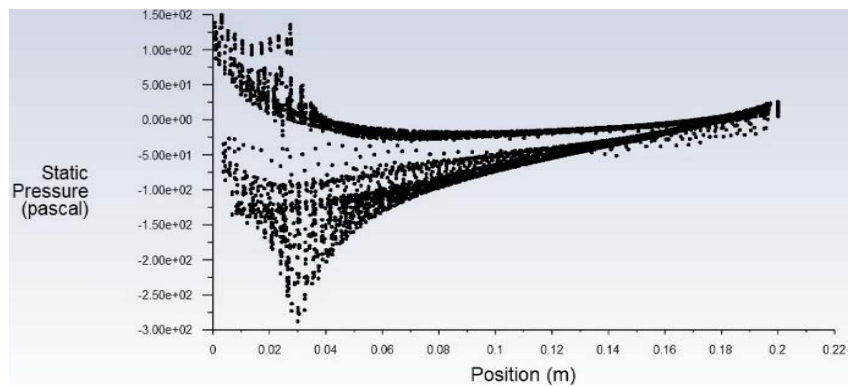


Fig. 7  $C_p$  vs  $x/c$  curve of the wavy wing simulated in the Venusian atmosphere

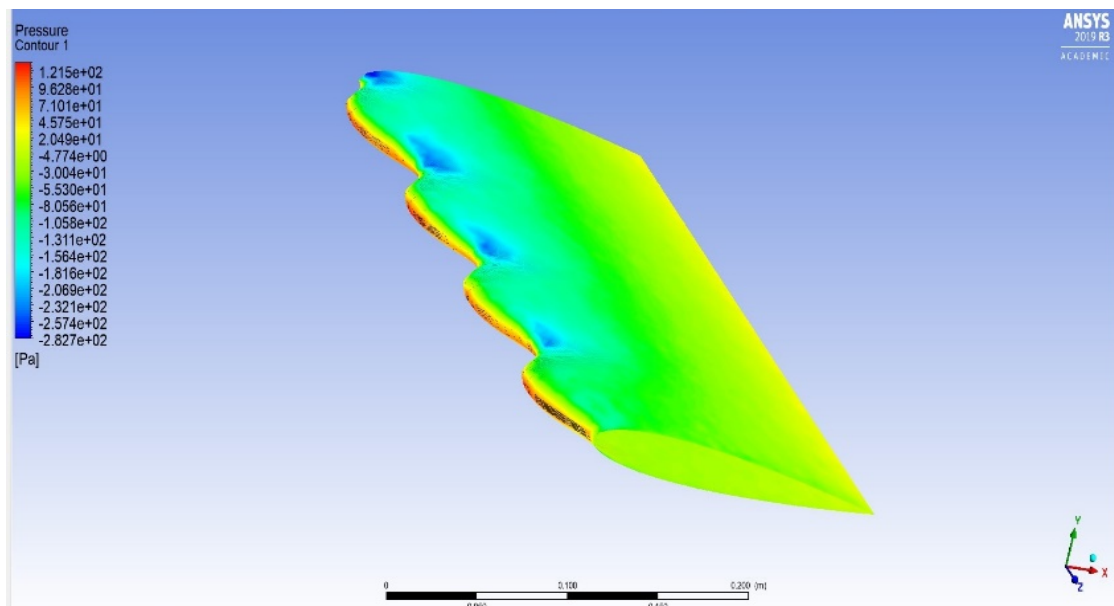


Fig. 8 Pressure contours on the wavy wing simulated in the Martian Atmosphere



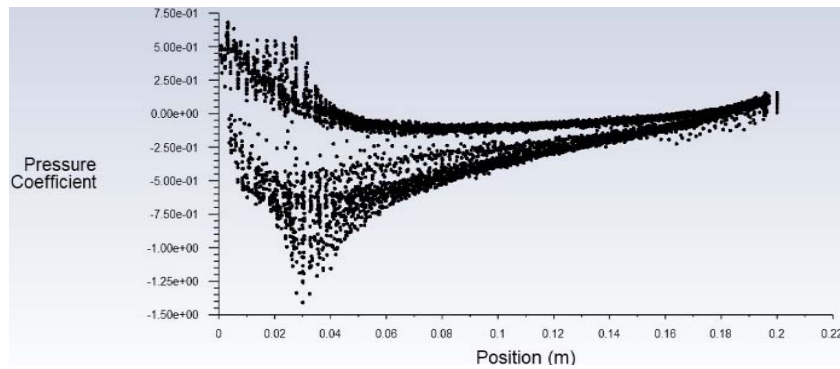
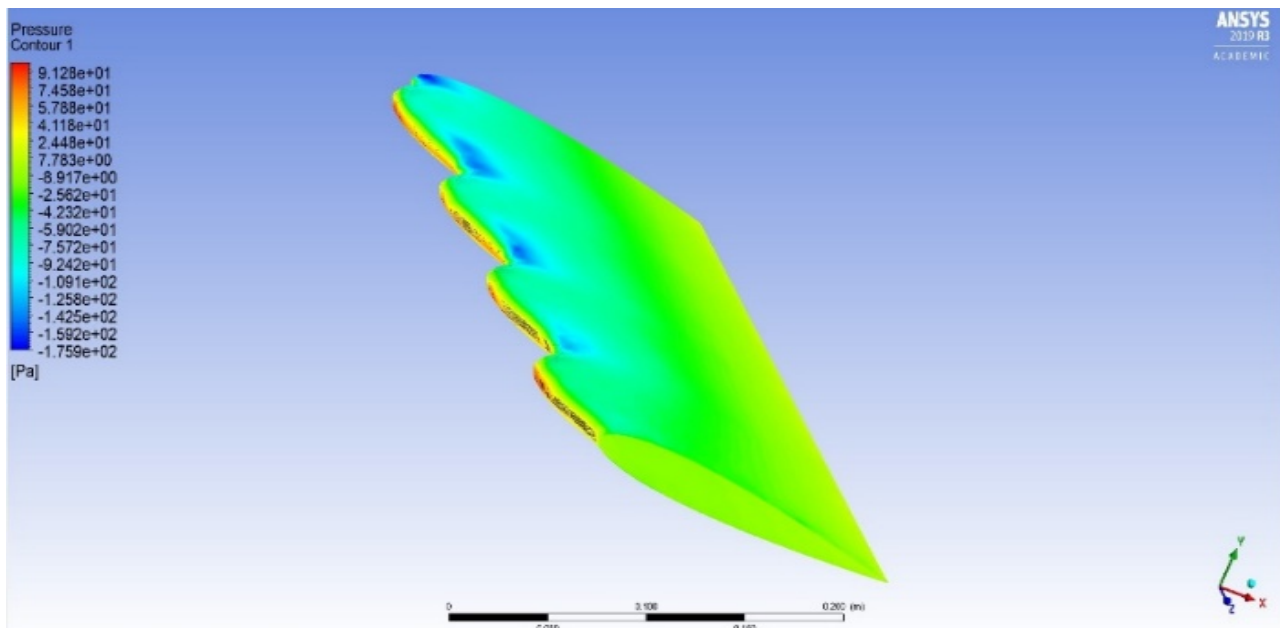
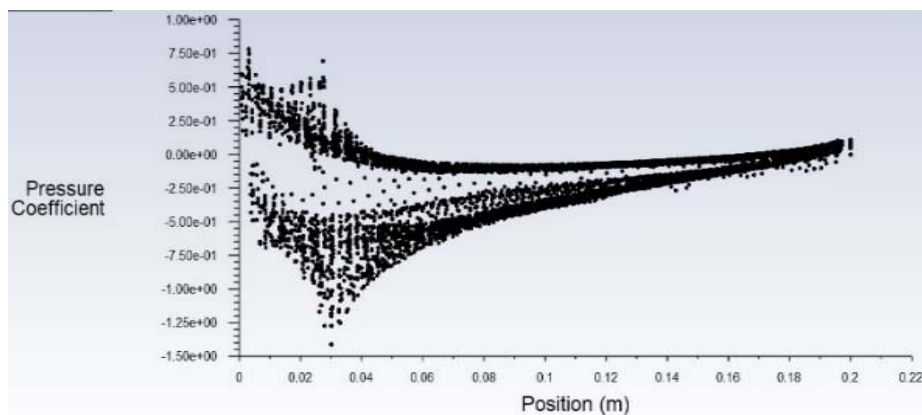
Fig. 9:  $C_p$  vs  $x/c$  curve of the wavy wing simulated in the Martian Atmosphere

Fig. 10 Pressure contours on the wavy wing in the Titan's atmosphere

Fig. 11  $C_p$  vs  $x/c$  curve of wavy wing in the Titan's atmosphere

### C. Titan

Titan provides a good analogue as a natural laboratory in which chemical and physical properties can be studied on a

planetary scale and help us understand early chemical evolution in the atmosphere of Earth. Titan has a thick atmosphere mainly consisting of nitrogen (94.2%) and

methane (5.65%). The atmosphere of titan is denser than the atmosphere of earth and hence the aerodynamic characteristics of the tubercle wing is changed to that on Earth. Fig. 10 shows the pressure distribution over the wavy wing in Titan's atmosphere. It can be observed from the contours that the pressure at the lower surface of the wing is high as compared to the upper surface thus producing lift. The region of low static pressures along the top of the wing depicted with the blue colour generate lifts but this taper off towards the tip of

wing and the trailing edge [6]. The stagnation region is displayed as a red just at the LE of the wing.

#### D. Uranus

The planet Uranus has the atmosphere composition of mainly hydrogen and helium with traces of methane. The simulation done with the similar gases produces the results as shown in Table III.

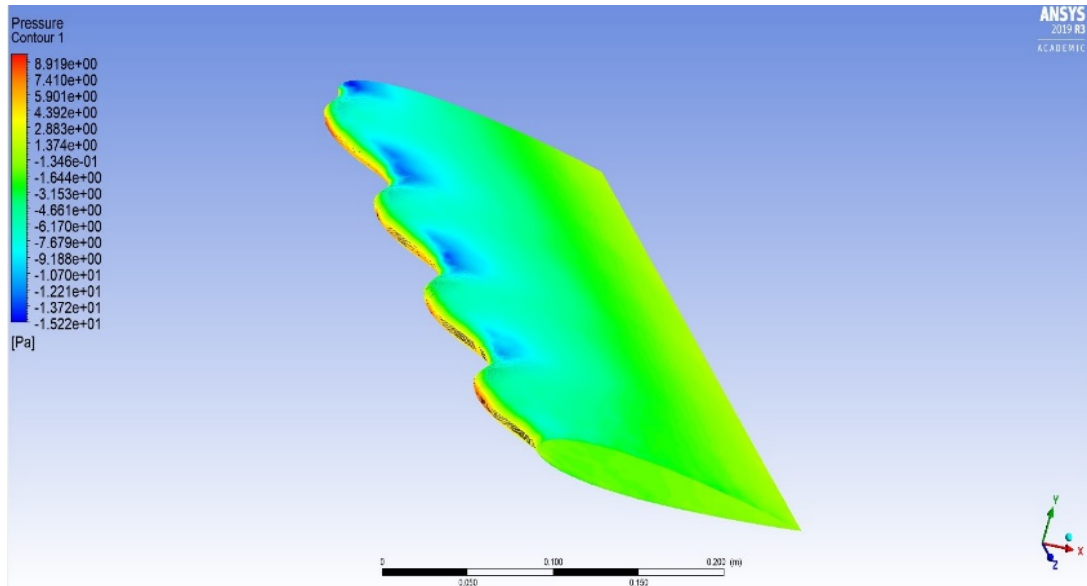


Fig. 12 Pressure contours on the wavy wing in the Uranus atmosphere

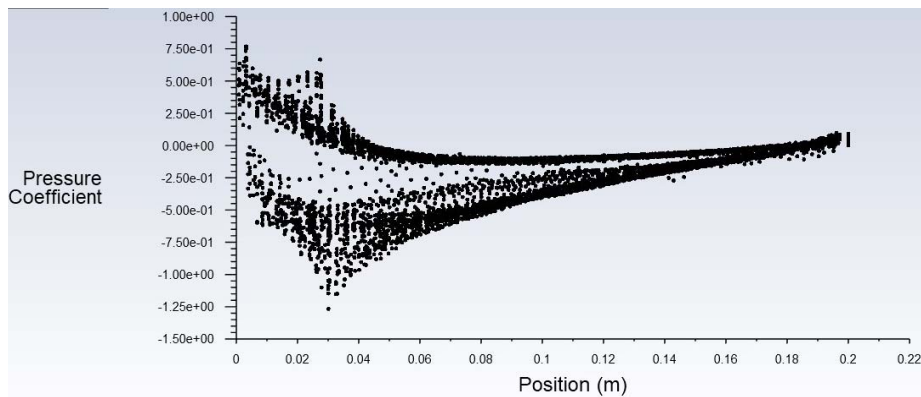


Fig. 13  $C_p$  vs  $x/c$  curve of wavy wing in the Uranus atmosphere

After simulating the wavy wing on the planetary bodies of our solar system, the different pressure contours were obtained. As a result, Table III also shows the value of lift coefficient and drag coefficient of NACA0012 wing with wavy LEs on the different planets at an angle of attack of  $5^\circ$ . As it can be explained from the table the atmosphere conditions of Saturn's Moon Titan are such that it generates more lift followed by the red planet Mars and Venus. The lift coefficient on the other planets is somewhat comparable and hence there is a possibility to use these wavy wings for the

unmanned aerial vehicles for planetary exploration.

TABLE III  
 $C_l$  AND  $C_d$  VALUES OF NACA0012 WAVY WING ON DIFFERENT PLANETARY ATMOSPHERES AT 5-DEGREE AOA

Planet	$C_l$	$C_d$
Venus	0.29166	0.03452
Mars	0.29809	0.03177
Titan	0.31028	0.03660
Uranus	0.28993	0.04882

## V.CONCLUSION

With the rise of the need for space exploration, the use of unmanned air vehicles for planetary exploration has also taken a sharp edge. The atmospheres on other planets are different than that of planet Earth which can drastically affect the flight conditions and hence the exploratory mission. In this paper an experimental study of using sinusoidal waves as the LE of the wing of UAVs has been done. Through previous done research on using wavy LE in the Earth's atmosphere showed that the lower effective angle of attack caused by the waviness is expected to lead to reduction in the lift. However, for higher  $Re$  where a sharp stall is observed, the stall may be delayed in portions of the wing, leading to a loss of lift before stall and an increase of lift in the post-stall [9]. Through the results obtained in this paper (Table III), it can be validated that at low subsonic speed of 15 m/s the coefficient of lift produced on Saturn's moon titan is the most as compared to the other planets. This comparative study between different planetary atmospheric characteristics on the effect of wavy wing can be used to design efficient fixed wing that will be capable to fly on different planets for exploratory missions.

## REFERENCES

- [1] Fish, F. E., and Battle, J. M., "Hydrodynamic Design of the Humpback Whale Flipper," *Journal of Morphology*, Vol. 225, 1995, pp. 51–60.
- [2] C. M. Jurasz and V. P. Jurasz, "Feeding modes of the humpback whale, *Megaptera novaeangliae*, in Southeast Alaska," *Sci. Rep. Whales Res. Inst.* 31, 69–83 (1979).
- [3] Johari, H., Henoch, C., Custodio, D., and Levshin, A., "Effects of Leading-Edge Protuberances on Airfoil Performance," *AIAA Journal*, Vol. 45, No. 11, 2007, pp. 2634-2641.
- [4] Guerreiro, J. L. E., and Sousa, J. M. M., "Low-Reynolds-Number Effects in Passive Stall Control Using Sinusoidal Leading Edges," *AIAA Journal*, Vol. 50, No. 2, 2012, pp. 461-469.
- [5] Watts, P. and Fish, F.E., The Influence of Passive, Leading Edge Tubercles on Wing Performance, *Unmanned Untethered Submersible Technology (UUST)*, Autonomous Undersea Systems Inst., Lee, NH, 2001.
- [6] Watts, P. and Fish, F.E., The Influence of Passive, Leading Edge Tubercles on Wing Performance, *Unmanned Untethered Submersible Technology (UUST)*, Autonomous Undersea Systems Inst., Lee, NH, 2001.
- [7] ANSYS. "Chapter 10. Modelling Turbulence Fluent Manual." 2001.
- [8] Fundamentals of Aerodynamics, John D. Anderson JR.
- [9] Direct numerical simulations of the flow around wings with spanwise waviness at a very low Reynolds number D. Serson, J.R. Meneghini B., S.J. Sherwin
- [10] Performance analysis of fixed wing space drones in different solar system bodies M. Hassanaliana, D. Ricea, S. Johnstoneb, A. Abdelkefia,
- [11] Physical parameters of the Martian Atmosphere, Basil Petropolous, C. Macris
- [12] <https://solarsystem.nasa.gov/solar-system/our-solar-system/overview/>
- [13] The effect of undulating leading-edge modifications on NACA0012 airfoil characteristics, N. Rostamzadeh, R. M. Kelso, B. B. Dally, and K. L. Hansen *Phys. Fluids* 25, 117101 (2013); doi: 10.1063/1.4828703
- [14] Bushnell, D. M. and Moore, K. J. (1991). Drag reduction in nature. *Ann. Rev. Fluid Mech.* 23, 65-79.